Available online at www.sciencedirect.com

ScienceDirect

Advances in Space Research 55 (2015) 1190–1198

ADVANCES IN SPACE RESEARCH (a COSPAR publication)

www.elsevier.com/locate/asr

On the use of Very Low Frequency transmitter data for remote sensing of atmospheric gravity and planetary waves

Sujay Pal [a,b,*], Suman Chakraborty [a], Sandip K. Chakrabarti [a,c]

[a] Indian Centre for Space Physics, 43 Chalantika, Garia St. Road, Kolkata 700084, India
[b] The University of Electro-Communication, Chofu, Tokyo 182-8585, Japan
[c] S. N. Bose National Centre for Basic Sciences, JD Block, Sector-III, Kolkata 700098, India

Received 21 July 2014; received in revised form 19 November 2014; accepted 21 November 2014
Available online 28 November 2014

Abstract

Continuous ground-based monitoring of Very Low Frequency (VLF) transmitter signals is an efficient remote sensing tool for studying of the lower ionosphere (60–90 km). Here, we present the use of VLF radio data to study short-period (~min–hrs) atmospheric gravity waves and long-period (~days) planetary waves. We analyse VLF data from several receiving stations obtained by ICSP-VLF network during the total solar eclipse of July, 2009 to show the existence of short-period atmospheric gravity waves. We find dominant wave periods range from 10 min to 1 h around the time of maximum eclipse phase which could be associated with atmospheric gravity waves excited due to the eclipse. We also analyse VLF amplitude data of 2007 received at ICSP, Kolkata from VTX (18.2 kHz) transmitter for planetary wave-type oscillations in the mesosphere–lower ionosphere system. Fourier and wavelet analysis show presence of periodic structures with periodicity in the range of 5–27 days. We compare VLF planetary spectrum with spectrum obtained from total column density of Ozone and mesospheric average temperature data which may indicate vertical coupling between the stratosphere and ionosphere in winter to early spring time.

Keywords: Atmospheric gravity waves; Planetary waves; Solar eclipse; D-region; Earth–ionosphere waveguide; VLF

1. Introduction

The upper atmosphere is in mechanical equilibrium with ionization forces of the Sun and Cosmic rays from above and forces from below including different types of atmospheric waves. Very Low Frequency (VLF) radio signals (3–30 kHz) from transmitters worldwide propagate globally while reflecting within a waveguide formed by the Earth-surface and upper mesosphere–lower ionospheric region (60–90 km). Reflected amplitude and phase of these waves contain information about all types of atmospheric forcing from below and the solar or other forcing from above. Thus VLF radio waves have become a very efficient remote sensing tool for this region.

Atmospheric waves (such as atmospheric gravity waves [AGW], planetary waves [PW], tidal waves) transfer energy and momentum from the lower atmosphere to the upper atmosphere and maintain atmospheric balance (Hines, 1960; Lastovicka, 1997; Lastovicka, 2001). Movement of the solar terminator during sunrise and sunset through the atmosphere, produces atmospheric gravity waves periodically at the mesosphere and thermosphere (Beer, 1978; Dungenbaeva and Ganguly, 2004; Antonova et al., 2006; Afraimovich, 2008). Irregularities and inhomogeneities in the atmosphere and ionospheric plasma produced by the sharp temperature gradient associated with the solar

* Corresponding author at: Indian Centre for Space Physics, 43 Chalantika, Garia St. Road, Kolkata 700084, India. Tel.: +91 33 2436 6003x21.
E-mail addresses: myselfsujay@gmail.com (S. Pal), suman.chakrabarty37@gmail.com (S. Chakraborty), sandip@csp.res.in (S.K. Chakrabarti).

http://dx.doi.org/10.1016/j.asr.2014.11.023
0273-1177/

terminator are responsible for the generation of atmospheric gravity waves (Somsikov and Ganguly, 1995). During a solar eclipse, the atmosphere experiences a virtual sunset and sunrise in quick succession, thus generation of GWs is expected. Study of such GWs would be interesting since their time of occurrence are known before the events. Chimonas and Hines (1970) were the first to suggest the generation of atmospheric GWs during a solar eclipse due to the disturbance of heat balance along supersonic travel of trajectory of the moon's shadow. Subsequent studies show that thermal cooling of the stratospheric Ozone layer during solar eclipses acts as a main source of GWs. First experimental evidence of the existence of GWs during solar eclipse was made by Walker et al. (1991), where waves with periods of 30–33 min were observed at ionosonde sounding virtual heights. Till date, all works on the study of existence of GWs during solar eclipses have been made by using GPS TEC, RADAR and ionosonde measurements (Afraimovich, 2008; Paul et al., 2011; Dutta et al., 2011; Sauli et al., 2007). For the first time, we use the VLF signal characteristics to study of the existence of GWs during solar eclipse and their effects on VLF signal. VLF data of Indian Centre for Space Physics (ICSP) during total solar eclipse of 22 July, 2009 were utilized to find wave-like oscillations associated with the eclipse.

Among the longer-period atmospheric waves, planetary waves (PWs) are characterized by periods of 2–30 days. Generally, PWs are not able to penetrate altitudes above 100–110 km due to atmospheric viscosity and other reasons (Lastovicka, 2006). Nevertheless, oscillations at PW periods were observed at all ionospheric layers (Pancheva and Haldoupis, 2002; Schmitter, 2011) and sometimes they are referred to as planetary wave-type oscillations (PWTOs). Travelling normal mode planetary waves of period around 2, 5, 10 and 16 days interact with other waves or zonal mean flow and govern dynamics of middle-atmosphere specially in winter time associated with Brewer–Dobson atmospheric circulation (Pancheva et al., 2008; Weber et al., 2011). There are many works which study the coupling mechanisms between stratosphere, mesosphere and lower thermosphere region via upward propagation of PWs (Liu and Roble, 2005; Bremer and Berger, 2002; Pancheva et al., 2008; Pancheva et al., 2009). Simultaneous occurrence of PWs in the lower ionosphere/upper mesosphere and stratosphere is a clear indicator of vertical atmospheric coupling between the two regions (Jacobi et al., 2007).

In this paper, we analyse the VLF amplitude data collected by ICSP-VLF network and total Ozone and temperature data of NASA satellite to study PWs and coupling phenomena in the mesosphere–lower ionosphere system. We show that measurement of sub-ionospheric reflected VLF wave amplitude can be used to study short-period atmospheric gravity waves as well as longer period planetary waves. We present results analysing the VLF data obtained during a solar eclipse as well as during nighttime of the year 2007. Organization of this paper is following. In Section 2, we show basic VLF data and data analysis procedure. In Section 3, we present results for gravity waves associated with the solar eclipse of July 22, 2009 and for planetary waves. In the last Section, we make concluding remarks.

2. VLF data analysis procedure

VLF data are taken from the ICSP-VLF network consisting of several receiving stations throughout India. Here we consider the propagation at frequency 18.2 kHz transmitted by the Indian VLF transmitter VTX3 (**lat**: 8.38°**N**, **long**: 77.75°*E*). Ionospheric reflected components of the signal induce e.m.f in the magnetic field loop antenna. Induced current is amplified and digitized by using a radio receiver and digital sound card to record desired signal amplitude for 24 h. In Fig. 1, we show all the four propagation paths: VTX-Kolkata (1946 km), VTX-Malda (2151 km), VTX-Raiganj (2207 km) and VTX-Kathmandu (2296 km) under investigation. In the first panel of Fig. 2, we show an example of standard diurnal variation of VTX (18.2 kHz) signal amplitude from Winter (January) to Summer (June) of 2007. Amplitude along the *Y*-axis is relative and is shifted by 10 dB to plot all data separately. Each diurnal variation is associated with two minima: one at around local sunrise time and other at around local sunset time. These two minima are called sunrise and sunset terminator times respectively. At dawn, as solar rays begin to pass through the atmosphere, they ionize the latter and this marks formation of ionospheric D-region. However, rate of recombination remains roughly equal to rate of ionization. This makes radio waves to be reflected from E-region, but now they have to travel through newly formed D-region. As a result, due to attenuation, signal strength is greatly decreased. As time goes on, more and more UV and soft X-ray photons from the Sun increases the rate of ionization in the D-region. VLF radio waves then start to reflect from the D-region with reduced reflection height. Thus received signal strength starts to increase and throughout the day time variation of signal strength follows the solar flux variation with solar zenith angle. At night, ions and neutrals in the D-region of the ionosphere recombine quickly with free electrons and as a result the D-region **almost** vanishes. This makes VLF radio waves to reflect again from the E-region.

For the purpose of this paper, we choose two sets of data for harmonic analysis. First, to analyse existence of small scale wave-like disturbances associated with atmospheric gravity waves, we choose VLF data set during total solar eclipse of July 22, 2009. ICSP organized a vast VLF campaign throughout India during the total solar eclipse of July 22, 2009 and collected VLF data from several places. Corresponding VLF data with effects from solar eclipse are published in Chakrabarti et al. (2010), Chakrabarti et al. (2012), Chakrabarti et al. (2012) and Pal et al. (2012), Pal et al. (2012). Here, we took the same

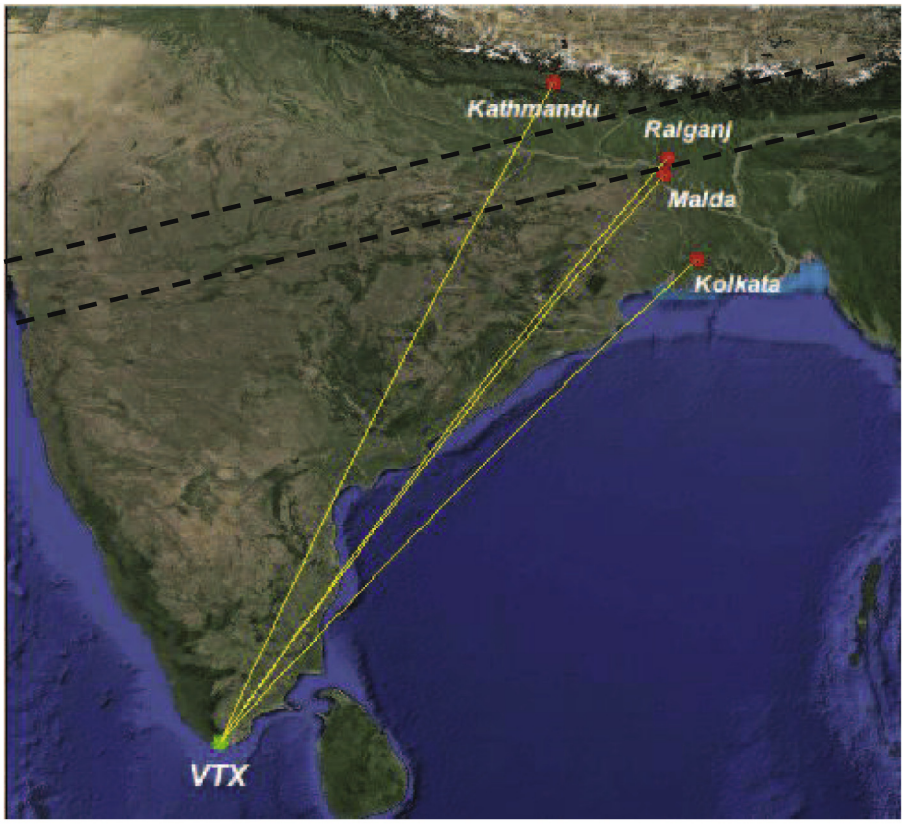

Fig. 1. Great circle paths between the transmitter VTX (18.2 kHz) and the four receivers under study. Black dotted lines show the approximate path of total solar eclipse belt on July 22, 2009.

VLF data from four places (shown in Fig. 1) for the analysis of gravity waves during solar eclipse period. We took 4 h data of normal and eclipse day starting from 4:00 am IST (=UT + 5:30) to 8:00 IST for AGW analysis. Solar eclipse period was approximately from 5:30 IST to 7:30 IST with maximum obscuration at around 6:30 ± 0:05 IST. 'Normal' unperturbed data are taken from July 21 and July 23, the day before and after the eclipse day.

In our next analysis, we choose whole year VLF amplitude data of 2007 (shown in second panel of Fig. 2) to look for large scale wave-like oscillations in the D-region associated with planetary waves. We have 270 days data out of 365 days. Missing days are identifiable from the second panel of Fig. 2. We took 2 h amplitude average in the diurnal curve at night (around local mid-night). Variation of this average nighttime VLF amplitude with day of the year serves as a proxy for planetary wave activities and is presented in first panel of Fig. 3. Second panel of Fig. 3 shows average variation of nighttime temperature (K) at 85 km altitude near the mesopause region over Kolkata for 2007. Third panel of Fig. 3 shows variation of total Ozone (column density) in Dobson unit over Kolkata for the same year. Nighttime temperature data are obtained from the SABER instrument on board the NASA's TIMED satellite (LEVEL2A data product from saber.gats-Inc.com). This temperature profile is obtained from the nearest orbits corresponding to the nighttime profile (13 UT to 22 UT) over an area $5^\circ \times 5^\circ$ around the receiver location at Kolkata. Connection between the daytime VLF amplitudes and temperatures around the mesopause region (Silber et al., 2013) prompted us to investigate the temperature fluctuations as a parameter for monitoring atmospheric forcing in the mesosphere from below. Ozone data is obtained from the Ozone Monitoring Instrument (OMI) on board the NASA's AURA spacecraft (OMI AURA Level 3 data from the website <http://disc.sci.gsfc.nasa.gov/Aura/>) with main contribution from the stratosphere. So Ozone data could be a potential parameter to study stratospheric wave activities. Any correlation of wave activities obtained from the Ozone, temperature and VLF data could be a direct evidence of coupling phenomena between the stratosphere and lower ionosphere/upper mesosphere.

We use both Fourier and wavelet analysis methods to look for hidden wave-like oscillations in VLF amplitude data. Morlet mother wavelet function is used to calculate wavelet power spectrum or periodogram, since it is suitable for analysis of atmospheric fluctuations (Kumar, 2007). We set minimum period of one minute during FFT and wavelet analysis for small scale wave-like disturbances while, we set minimum period of one day for large scale wave-like disturbances with second set of data.

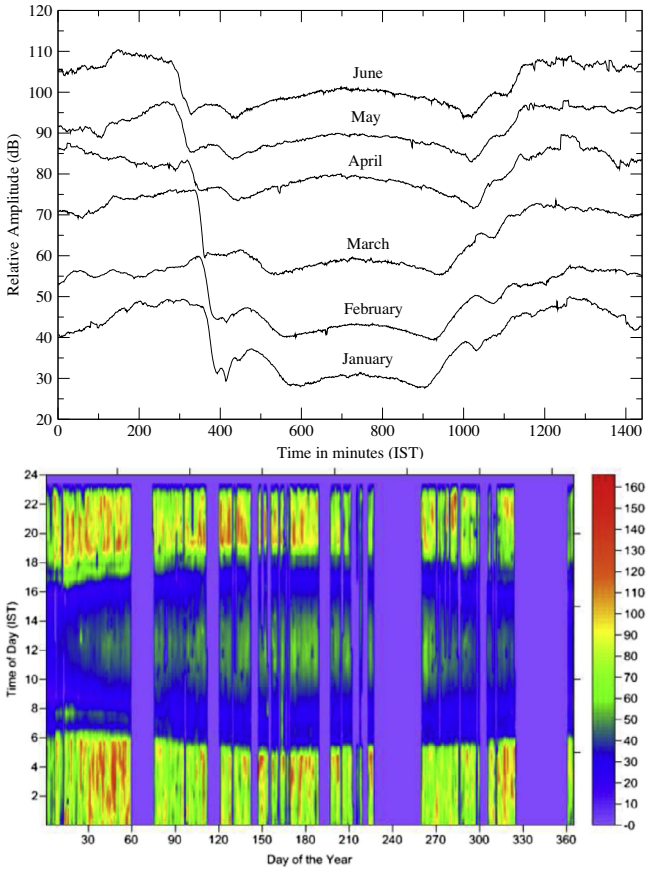

Fig. 2. Standard diurnal variation of the VTX (18.2 kHz) signal amplitude as it changes from Winter (January) to Summer (June) (first panel) and the diurnal variation for the whole year of 2007 (second panel).

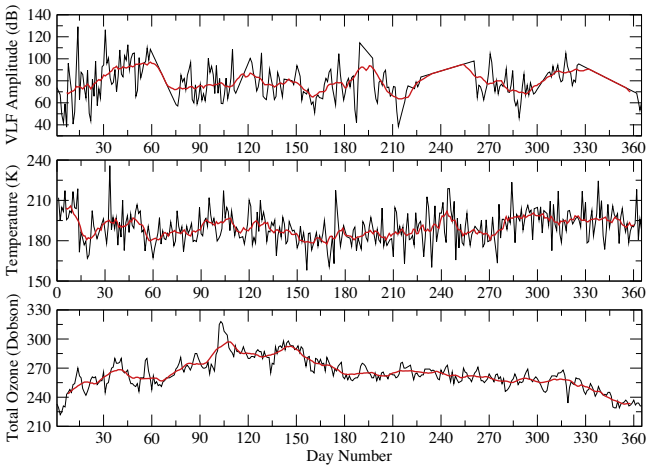

Fig. 3. Variation of average nighttime VLF amplitude in dB (top panel), SABER temperature in K at 85 km altitude (middle panel) and total column density of Ozone (lower panel) in Dobson unit with time of the year 2007 over Kolkata region. Red curves represent 15 days running average. (For interpretation of the references to color in this figure legend, the reader is referred to the web version of this article.)

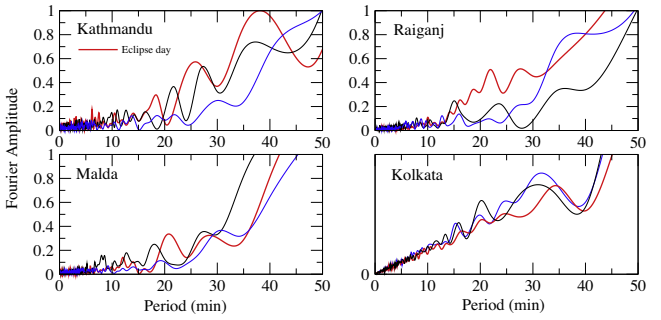

Fig. 4. Normalized FFT spectrum corresponding to three days: the day before solar eclipse (black), solar eclipse day (red) and the day after solar eclipse (blue) at Kathmandu, Raiganj, Malda and Kolkata respectively. All three places (Kathmandu, Raiganj and Malda) show an enhancement of power spectra on 22 July 2009 than on control days, while Kolkata shows a reduction in power spectra on the eclipse day. (For interpretation of the references to color in this figure legend, the reader is referred to the web version of this article.)

3. Results

3.1. Small scale atmospheric gravity waves

We now present our results of Fourier and wavelet analysis of VLF data corresponding to solar eclipse and normal conditions. Fig. 4 shows normalized FFT spectrum of VLF signals at four places corresponding to three days: the day before solar eclipse (black), solar eclipse day (red) and the day after solar eclipse (blue). Out of this four places, Raignaj was inside the eclipse totality belt and experienced 100% obscuration during maximum eclipse phase. Kathmandu experienced ~96.3% and was (~200 km) far from the totality belt. While Malda was nearly within the totality belt, Kolkata was far away from the totality and experienced only about 90% of solar obscuration. We see that except Kolkata, other three places have gone through much higher wave-like oscillations (with periods ranging from 10–40 min) on the solar eclipse day as compared to a normal day. These wave-like oscillations are clearer specially for Kathmandu and Raiganj. If we look into wavelet power spectrum of VLF amplitude deviation data (obtained by subtracting normal day from eclipse day VLF data) for these two places (Fig. 5), we see that in Kathmandu (a), most of the wave periods 10 min to ~1 h are concentrated at the time of maximum solar eclipse obscuration (~6:30 IST), while in Raignaj (c) much of the wave activities are within 5:00 to 5:20 IST before the eclipse. Wave activity is lower during the eclipse time period (5:30–7:30 IST) with periods ranging from 20 min to ~1 h. The scale average wavelet powers over the 10–60 min band for both places are shown in Fig. 5(b) and (d). Strong significant peak above the 95% confidence level (dashed line) can be seen clearly for Kathmandu receiver around the eclipse maximum time (6:30 AM), while the variances are low for Raiganj compared to the variances associated with the sunrise terminator. It is worth mentioning that solar terminators generate atmospheric gravity waves in the atmosphere regularly and could exist up to 1 h. Sunrise time at Raiganj on eclipse day was 4:59 IST. So the strong wave fluctuations between 5:00 and 5:20

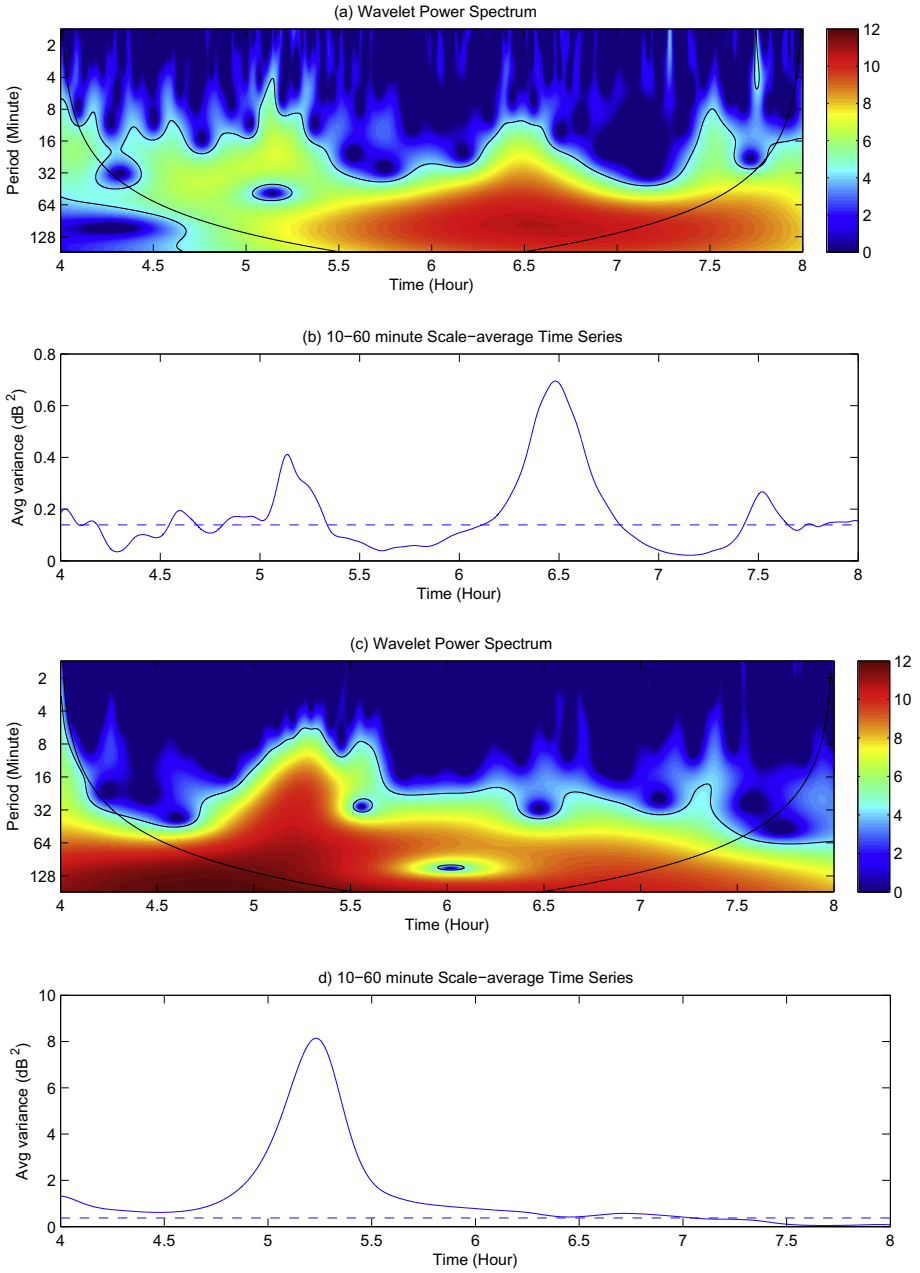

Fig. 5. The Wavelet power spectrum of deviations of the VLF amplitudes due to solar eclipse on 22 July, 2009 for Kathmandu (a) and Raiganj (c) receiving stations. The cone of influence, where zero padding has reduced the variance and the 95% confidence line (thick contour) are shown in the wavelet spectrum. The sunrise time and the time of maximum eclipse phase for both the places were around the time of 5:00 AM and 6:30 AM respectively. (b) and (d) are the scale-average wavelet powers over the 10–60 min band for the sites respectively. The dashed lines are the 95% confidence lines. Periodic wave structures with period ranging from 10 min to ~1 h as evidenced by high power density can be seen.

IST at Raiganj could be associated with the sunrise terminator generated gravity waves. In Fig. 6, we present wavelet power spectrum of the VLF amplitude deviation data due to the eclipse at Malda (a) and Kolkata (c) having maximum obscuration 99.6% and 89.9% respectively. Fig. 6(b) and (d) show the scale average wavelet powers over the 10–60 min band for both places respectively, where less dominated wave periods during eclipse time than around the sunrise time can be seen. In general, the presence of strong wave periods during the solar eclipse phase shows excitements of atmospheric gravity waves generated due to the movement of moon's shadow on Earth's atmosphere during the solar eclipse.

3.2. Large scale planetary waves

In this subsection, we present wave-like periodic structures in the year long VLF, Ozone and mesospheric temperature data associated with planetary wave-type oscillation suggesting a stratosphere to mesosphere

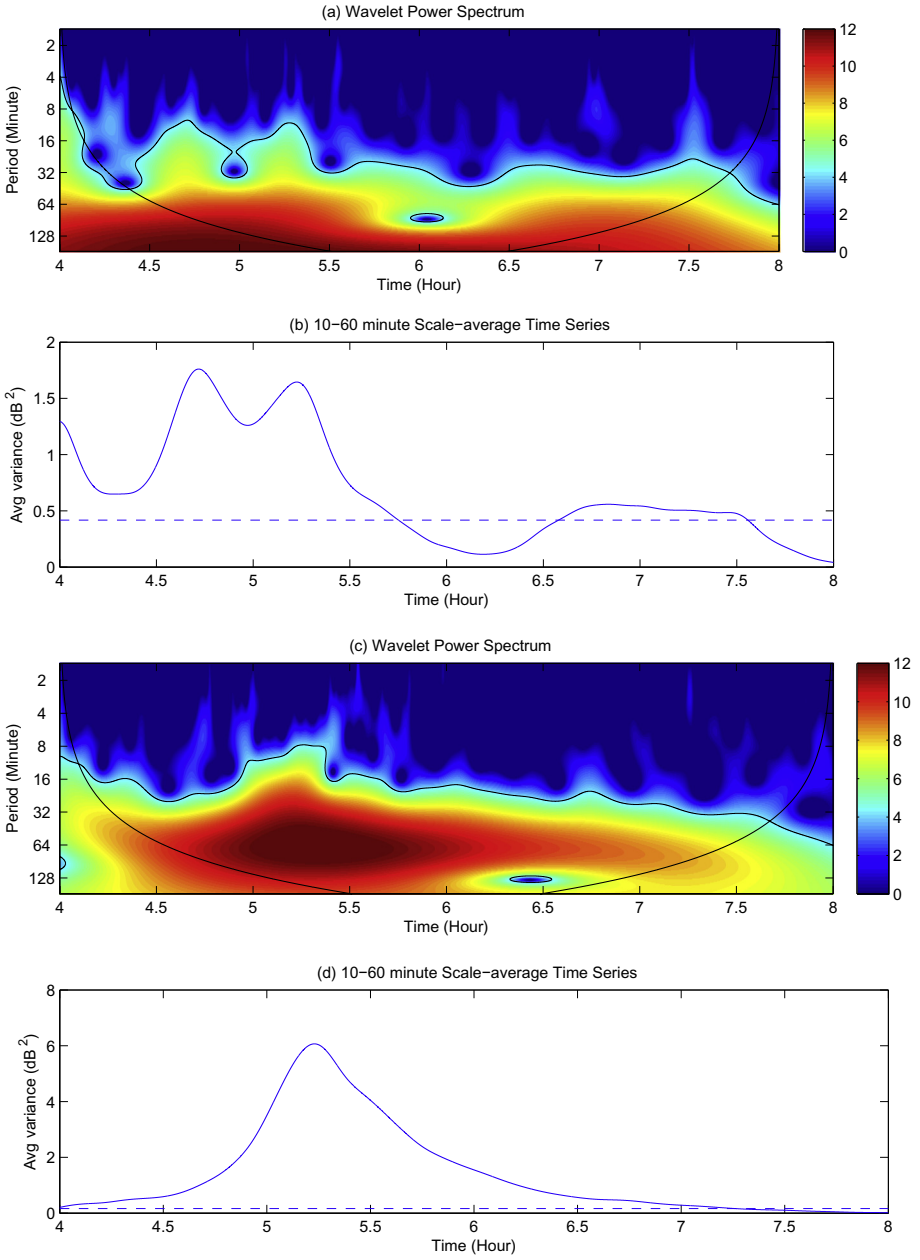

Fig. 6. The wavelet power spectrum of VLF the amplitude deviations for Malda (a) and Kolkata (c) receiving stations. (b) and (d) are the scale-average wavelet powers over the 10–60 min band. The dashed lines are the 95% confidence lines. The sunrise time and the time of maximum eclipse phase were around the time of 5:00 AM and 6:30 AM respectively.

coupling at least in winter to early spring time span. Planetary wave spectrum for 2007 is shown in Fig. 7. Peaks in top panel show Fourier amplitude of planetary wave-like oscillations corresponding to VLF amplitude data, middle and bottom panels show same variations for temperature and total Ozone data respectively. In VLF spectrum, wave periods of 12–14, 16–18, 22 and 27 days could be visible. We find periods of 12–14, 17–19, 22 and 25 days in SABER temperature data, while in Ozone data we find extended peaks at 13, 16, 22 and 26.5 days. Dominant and strongest 27-day period in the VLF spectrum could be related to the 27-day variability of solar irradiance. To illustrate occurrence times for different periodic structures associated with planetary wave activities, we present wavelet analysis results in Fig. 8. This analysis has been done with data from Fig. 3 and hence top, second and third panels represent wavelet spectrum of VLF, SABER temperature and total Ozone data respectively. With VLF wavelet spectrum we see that persistent 12–20 days wave periods are concentrated in January–April and also during June–July and September. From the SABER temperature spectrum 16–35 days are seen within January–March. From wavelet spectrum of Ozone data presented, we can see that almost all the planetary wave-type oscillations occurred in winter

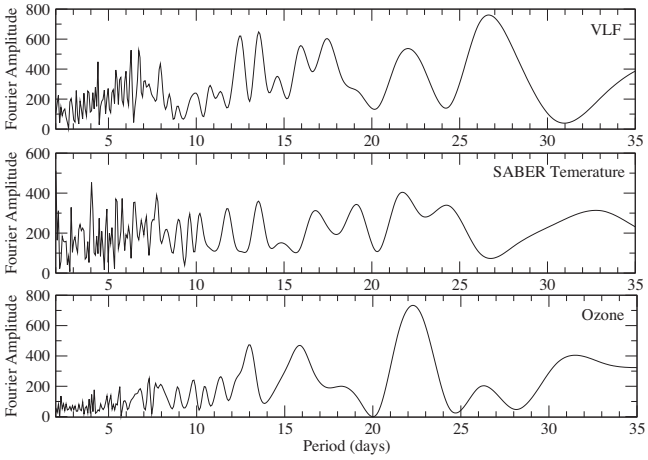

Fig. 7. Planetary FFT spectrum obtained respectively from VLF (top panel), temperature (middle panel) and O3 (bottom panel) data.

to spring (January–April, 2007). While there exists summer time wave activities in VLF data, there are less wave events or almost no periodic events in Ozone data during autumn or summer. One of the reasons behind this is that mean zonal flow in summer is not transparent to planetary waves and their propagation is suppressed by summer stratospheric wind (Lastovicka, 2006). During winter in Northern hemispheric tropical region, strength of Brewer–Dobson atmospheric circulation increases with the increase of upward mass flux from troposphere to stratosphere (Holton, 1990). Strong Brewer–Dobson circulation mainly associated with atmospheric planetary waves in winter time might help in atmospheric coupling process between the stratosphere and upper mesosphere (Weber et al., 2011; Jacobi et al., 2007). The last panel of Fig. 8 shows the geomagnetic Kp index for the year 2007. Geomagnetic storms, indicated by a Kp of 5 or higher, have very little effects on the radio propagation at equatorial region. Also, very recently, it has been shown by Kumar and Kumar (2014) that moderate geomagnetic storms have no effects on low latitude VLF propagation paths during solar minimum period. Thus the effects from the geomagnetic storms on the low-latitude VTX-Kolkata path can be neglected for the solar minimum year of 2007.

In Fig. 9, we present the time evolution of the amplitudes of 10-day (a), 16-day (b), 10–20 day (c) and 27-day (d) planetary waves for VLF (solid curve), mesopause temperature (dotted curve) and Ozone density (dashed curve) respectively. Some similarity of wave-like oscillations specially of 10-day component in Ozone and VLF and 16-day component in Ozone and mesopause temperature during winter to spring may give an indication of vertical atmospheric coupling process. It is also to be mentioned here that high anti-correlation between the day-time VLF amplitudes and mesopause temperature has been reported by Silber et al. (2013), where most of the propagation paths were over the mid-latitude region. Here, we have found small positive correlation correlation ($r = 23\%$) between

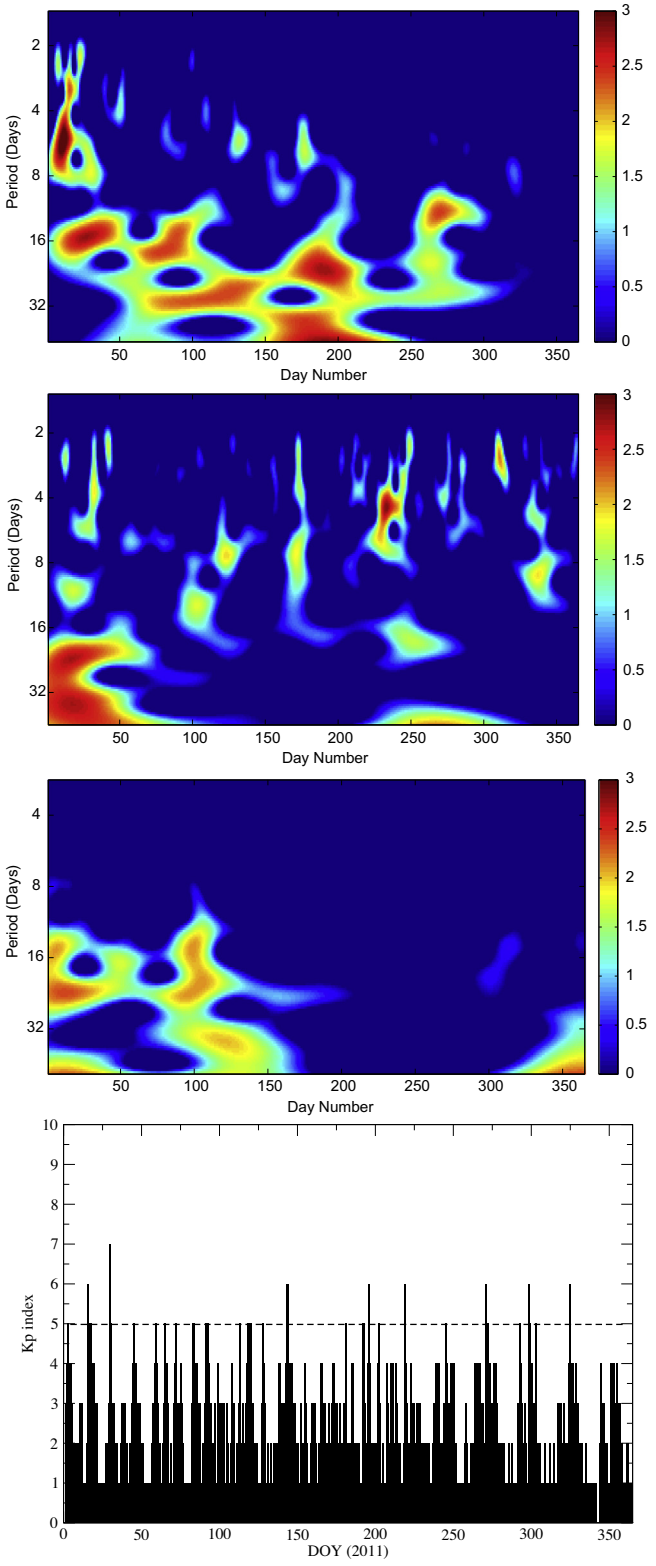

Fig. 8. Time–frequency wavelet power spectrum obtained respectively from the VLF (first panel), mesopause temperature (second panel) and total O3 (third panel) data are shown in this figure. The geomagnetic Kp index for the year has been shown in the last panel.

the VLF nighttime amplitude and temperature variation around the mesopause region (85 km) and small negative correlation coefficient with total Ozone ($r = -33\%$)

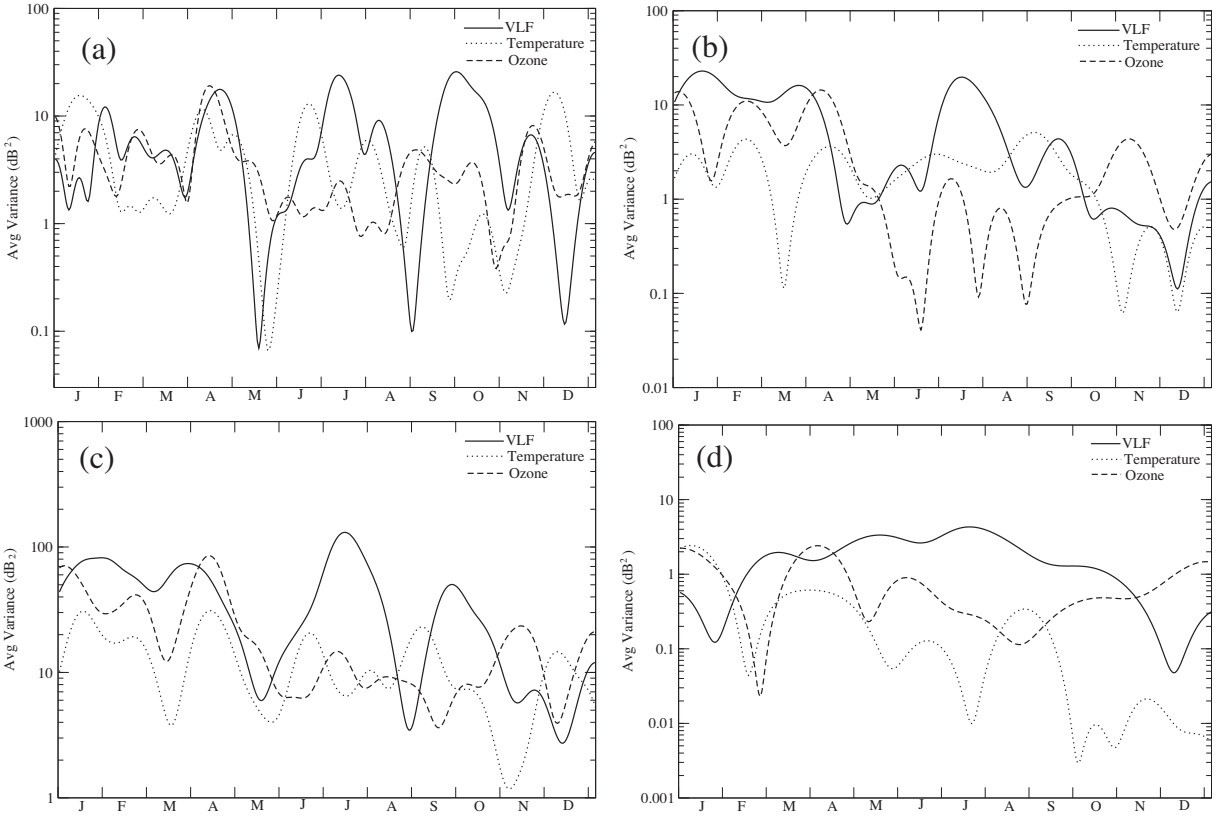

Fig. 9. Time evolution of scale average wavelet power of the amplitudes of 10-day (a), 16-day (b), 10–20 day (c) and 27-day (d) planetary waves for VLF (solid curve), mesopause temperature (dotted curve) and Ozone density (dashed curve) respectively.

throughout the year. However, the latitude dependence of the connection between the VLF amplitudes and other atmospheric parameters is subject to more investigations.

4. Conclusions

We present the use of VLF amplitude data for the study of both short-period and longer-period atmospheric waves. Presence of gravity waves triggered by the solar eclipse is very clear in data obtained from Kathmandu receiving station which was ~200 km away from totality zone of eclipse. Since solar eclipse of July, 2009 was just after the sunrise, clear identification of wave periods of gravity waves due to the eclipse alone become very difficult for some of receiving places (especially where eclipse was not total) because of interferences among weaker waves generated due to solar eclipse and strong waves by sunrise terminator. On the other hand, periodic structures in Ozone data associated with planetary waves are mostly found in winter to early spring time of the year. The periodic structures of planetary waves in the VLF data are found almost throughout the year. Some similarity in wave-activities of 10-day PW in Ozone and VLF data and similarity in wave activities of 16-day component between Ozone and mesopause temperature at least in winter to spring time may suggest coupling among the stratosphere–mesosphere–lower thermosphere system. Thus continuous monitoring of VLF transmitter can be a very efficient remote sensing tool to study all types of atmospheric forcing from below. This adds an extra perspective to the study of atmosphere–ionosphere coupling.

Acknowledgments

The authors thank to the Ministry of Earth Science for providing financial support towards this research and acknowledge the NASA for the SABER and OMI-O3 data sets.The authors also appreciate comments and suggestions expressed by all the reviewers.

References

Afraimovich, E.L., 2008. First GPS-TEC evidence for the wave structure excited by the solar terminator. Earth Planets Space 60, 895–900.

Antonova, V.P., Dungenbaeva, K.E., Zalizovskii, A.V., Inchin, A.S., Kryukov, S.V., Somsikov, V.M., Yampolskii, Yu.M., 2006. Difference between the spectra of acoustic gravity waves in daytime and nighttime hours due to nonequilibrium effects in the atmosphere. Geomag. Aeron. 46 (1), 101–109.

Beer, T., 1978. On atmospheric wave generation by the terminator. Planet. Space Sci. 26, 185–189.

Bremer, J., Berger, U., 2002. Mesospheric temperature trends derived from ground-based LF phase-height observations at mid-latitudes: comparison with model simulations. J. Atmos. Sol. Terr. Phys. 64 (7), 805–816.

Chakrabarti, S.K., Sasmal, S., Pal, S., Mondal, S.K., 2010. Results of VLF campaigns in summer winter and during solar eclipse in indian succontinent and beyond, propagation effects of very low frequency radio waves. AIP 1286, 61–76.

Chakrabarti, S.K., Mondal, S.K., Sasmal, S., Pal, S., Basak, T., Chakrabarti, S., Bhoumik, D., Ray, S., Choudhury, A.K., Maji, S., Nandi, A., Yadav, V., Kotoch, T.B., Khadka, B., Giri, K., Gorain, S.K., Patra, N.N., Iqbal, N., 2012. VLF signals in summer and winter in the Indian sub-continent using multi-station campaigns. Indian J. Phys. 86 (5), 323–334.

Chakrabarti, S.K., Pal, S., Sasmal, S., Mondal, S.K., Ray, S., Basak, T., Maji, S.K., Khadka, B., Bhowmick, D., Chowdhury, A.K., 2012. VLF campaign during the total eclipse of July 22nd, 2009: observational results and interpretations. J. Atmos. Sol. Terr. Phys. 86, 65–70.

Chimonas, G., Hines, C.O., 1970. Atmospheric gravity waves induced by a solar eclipse. J. Geophys. Res. 75 (4), 875.

Dungenbaeva, K.E., Ganguly, B., 2004. Radiation changes in atmospheric wave dynamics and spectra. Math. Comput. Simul. 67, 411–417.

Dutta, G., Vinay, Kumar P., Venkat, Ratnam M., Mohammad, S., et al., 2011. Response of tropical lower atmosphere to annular solar eclipse of 15 January, 2010. J. Atmos. Sol. Terr. Phys. 73, 1907–1914.

Hines, C.O., 1960. Internal atmospheric gravity waves at ionospheric heights. Can. J. Phys. 38, 1441–1481.

Holton, J.R., 1990. On the global exchange of mass between the stratosphere and troposphere. J. Atmos. Sci. 47, 392–395.

Jacobi, C., Jakowski, N., Pogoreltsev, A., Frhlich, K., Hoffmann, P., Borries, C., 2007. The CPW-TEC project: planetary waves in the middle atmosphere and ionosphere. Adv. Radio Sci. 5, 393–397.

Kumar, K.K., 2007. VHF radar investigations on the role of mechanical oscillator effect in exciting convectively generated gravity waves. Geophys. Res. Lett. 34, L01803. http://dx.doi.org/10.1029/2006GL027404.

Kumar, A., Kumar, S., 2014. Space weather effects on the low latitude D-region ionosphere during solar minimum. Earth Planets Space 66, 76, <http://www.earth-planets-space.com/content/66/1/76>.

Lastovicka, J., 1997. Observations of tides and planetary waves in the atmosphere–ionosphere system. Adv. Space Res. 20 (6), 1209–1222.

Lastovicka, J., 2001. Effects of gravity and planetary waves on the lower ionosphere as observed from radio wave absorption measurements. Phys. Chem. Earth 26, 381–386 (Part C).

Lastovicka, J., 2006. Forcing of the ionosphere by waves from below. J. Atmos. Sol. Terr. Phys. 68, 479–497.

Liu, H.L., Roble, R.G., 2005. A study of a self-generated stratospheric sudden warming and its mesospheric/lower thermospheric impacts using coupled TIME-GCM/CCM3. J. Geophys. Res. 107 (D23), 4695. http://dx.doi.org/10.1029/2001JD001533.

Pal, S., Chakrabarti, S.K., Mondal, S.K., 2012. Modeling of sub-ionospheric VLF signal perturbations associated with total solar eclipse 2009, in Indian subcontinent. Adv. Space Res. 50, 196–204.

Pal, S., Maji, S.K., Chakrabarti, S.K., 2012. First ever VLF monitoring of lunar occultation of a solar flare during the 2010 annular solar eclipse and its effects on the D-region electron density profile. Planet. Space Sci. 73, 310–317.

Pancheva, D., Haldoupis, C., 2002. Planetary waves and midlatitude sporadic E layers: strong experimental evidence for a close relationship. JGR 107 (A6). http://dx.doi.org/10.1029/2001JA000212.

Pancheva, D., Mukhtarov, P., Mitchell, N.J., Merzlyakov, E., Smith, A.K., Andonov, B., Singer, W., Hocking, W., Meek, C., Manson, A., Murayama, Y., 2008. Planetary wave coupling (5–6-day waves) in the low-latitude atmosphere–ionosphere system. J. Atmos. Sol. Terr. Phys. 70 (1), 101–122.

Pancheva, D., Mukhtarov, P., Andonov, B., 2009. Global structure, seasonal and interannual variability of the migrating semidiurnal tide seen in the SABER/TIMED temperatures (2002–2007). Ann. Geophys. 27, 687–703.

Paul, A., Das, T., Ray, S., Das, A., Bhowmick, D., DasGupta, A., 2011. Response of the equatorial ionosphere to the total solar eclipse of 22 July 2009 and annular eclipse of 15 January 2010 as observed from a network of stations situated in the Indian longitude sector. Ann. Geophys. 29, 1955–1965.

Sauli, P., Roux, S.G., Abry, P., Boska, J., 2007. Acoustic-gravity waves during solar eclipses: detection and characterization using wavelet transforms. J. Atmos. Sol. Terr. Phys. 69 (2007), 2465–2484.

Schmitter, E.D., 2011. Remote sensing planetary waves in the midlatitude mesosphere using low frequency transmitter signals. Ann. Geophys. 29, 1287–1293.

Silber, I., Price, C., Rodger, Craig J., Haldoupis, C., 2013. Links between mesopause temperatures and ground-based VLF narrowband radio signals. JGR 118 (10), 4244–4255.

Somsikov, V.M., Ganguly, B., 1995. On the formation of atmospheric inhomogeneities in the solar terminator region. J. Atmos. Sol. Terr. Phys. 57, 1513–1523.

Walker, G.O., Li, T.Y.Y., Wong, Y.W., Kikuchi, T., Huang, Y.N., 1991. Ionospheric and geomagnetic effects of the solar eclipse of 18 March 1988 in East-Asia. J. Atmos. Sol. Terr. Phys. 53 (1–2), 25–37.

Weber, M., Dikty, S., Burrows, J.P., Garny, H., Dameris, M., Kubin, A., Abalichin, J., Langematz, U., 2011. The Brewer–Dobson circulation and total ozone from seasonal to decadal time scales. Atmos. Chem. Phys. 11, 11221–11235. http://dx.doi.org/10.5194/acp-11-11221-2011.